11-30-2011

Proteomic 2-D DIGE profiling of human vascular endothelial cells exposed to environmentally relevant concentration of endocrine disruptor PCB153 and physiological concentration of 17β-estradiol

Quentin Felty
Department of Environmental Health Sciences, Florida International University, feltyq@fiu.edu

Published in final edited form as:
Cell Biol Toxicol. 2011 February ; 27(1): 49–68. doi:10.1007/s10565-010-9170-6.

Proteomic 2-D DIGE profiling of human vascular endothelial cells exposed to environmentally relevant concentration of endocrine disruptor PCB153 and physiological concentration of 17β-estradiol

Quentin Felty
Department of Environmental & Occupational Health, Florida International University, Miami, FL, USA.

Abstract

Considering the recent studies that question previously reported cardio-protective effects of estrogen, there is a growing concern that endocrine disruptors may also contribute to the pathology of cardiovascular disease (CVD). The endocrine disruptor PCB153 has been reported to bind the estrogen receptor, induce vessel formation, and increase the formation of reactive oxygen species (ROS) in endothelial cells. Since PCB153 induced phenotypic changes are similar to estradiol, we postulated that PCB153 activates redox signaling pathways common to 17β-estradiol. Whether the effect of PCB153 on the proteome is comparable to 17β-estradiol is not known. Therefore we investigated the proteome of human microvascular endothelial cells (HMVEC) exposed to PCB153. Using 2-D DIGE coupled to MALDI-TOF/TOF MS, we found 96 protein spots significantly (greater than 1.5 fold) modulated by experimental treatments. Mass spectrometry identified 11 of 13 protein spots with high confidence protein score C.I. that was greater than 95%. Of the identified proteins, lamin A/C and far upstream element-binding protein (FUBP1) were regulated similarly by both treatments. FUBP1 is of particular interest because it controls c-myc. While lamin A/C modulates transcription factor AP-1 function. Interestingly, both c-myc and AP-1 are redox sensitive transcription factors known to regulate genes required for cell growth. Network analysis of these proteins showed transforming growth factor β-1 (TGFB1) and c-myc to play central roles. While our findings do not reveal any mechanisms involved in PCB153 induced vascularization, the identified network does provide a potential target pathway for further mechanistic studies of these relationships.

Keywords

endocrine disruptors; estrogen; endothelial cells; PCB153; proteomics; vascular lesion

Introduction

Pulmonary arterial hypertension (PAH) causes an increase in pulmonary arterial pressure that leads to right ventricular failure and death. In the United States, PAH afflicts approximately 100,000 individuals and causes 20,000 deaths each year (Hyduk et al. 2005). Vascular lesions of severe PAH consist of actively proliferating endothelial cells that lead to arterial blockage (Sakao et al. 2009). In women PAH is roughly twice as common compared to men (Newman et al. 2004); whether this occurrence may be attributed to the hormone

Address of corresponding author. Quentin Felty, Ph.D. Department of Environmental & Occupational Health Florida International University 11200 SW 8th Street, HLS 593 Miami, FL 33199 Feltyq@fiu.edu Phone: (305) 348-7785 Fax: (305) 348-4901.

estrogen is not clear. Recent studies question previously reported beneficial effects of estrogen on the cardiovascular system. The Women's Health Initiative, indicated that long-term use of estrogen did not decrease, and may have increased, the risk of cardiovascular disease (CVD) (Rossouw 2005). Both pulmonary hypertension and pulmonary intimal vascular lesions have been associated with the use of oral contraceptives (Irey and Norris 1973;Kleiger et al. 1976). Since estrogen is a known mitogen of endothelial cells, we postulate that pulmonary vascular lesions are a consequence of excess or unopposed estrogen. Although beneficial effects of estrogen on the endothelium have been reported (Cid et al. 2002); we propose that differences between endothelial cell types may account for greater susceptibility of pulmonary arteries to estrogen-induced vascular lesion formation.

Widespread contaminants in the environment such as arsenic, tobacco smoke, and polychlorinated biphenyls (PCBs) have been reported to possess estrogenic activity (Bitman and Cecil 1970;Davey et al. 2007;Meek and Finch 1999;Tavolari et al. 2006). There is now increasing evidence that exposure to these endocrine disruptors may contribute to the development of cardiovascular disease. Considering the recent studies that question the previously reported cardio-protective effects of estrogens, there is a growing concern that estrogenic PCBs may increase the risk for PAH by inducing the formation of pulmonary vascular lesions. The present study aims to investigate the differential effects on the proteome of human vascular endothelial cells exposed to environmentally relevant concentrations (ppb) of PCB153, and physiological concentrations of 17β-estradiol.

Materials and methods

Cell Culture

A telomerase-immortalized human microvascular endothelium (TIME) cell line was obtained from American Type Culture Collection (Manassas, VA) to be referred throughout this study as HMVEC. These endothelial cells have retained many of the phenotypic characteristics of the primary endothelial cells from which they were derived including normal cell morphology and the capacity to form tubules in vitro (Venetsanakos et al. 2002). Cells were grown in Endothelial Cell Basal Medium-2 (EBM-2) supplemented with EGM 2-MV Single-Quots from Lonza (Walkersville, MD). Estrogen treatments were studied under the following culture conditions: 75–80% confluent cultures were washed and serum starved in phenol red-free medium for 3h. Thereafter, the cells were treated with either PCB153 or 17β-estradiol in phenol red-free medium supplemented with 10% charcoal/dextran-treated fetal bovine serum to avoid any estrogenic activity and maintained for 24 hours.

Estrogenic chemical treatments

Stock solutions of PCB153, and 17β-estradiol were prepared in dimethyl sulfoxide (DMSO). The same amount of DMSO as in PCB and estradiol-treated cells were added to control cultures. The level of DMSO in experimental media was less than 0.1%. PCB congener 2,2′, 4,4′,5,5′-hexachlorobiphenyl (PCB153) was purchased from AccuStandard (New Haven, CT) and dissolved in DMSO. All other chemicals and reagents were purchased from Sigma (St. Louis, MO).

2D-DIGE (two-dimensional difference in gel electrophoresis)

Preparation of samples: Protein lysates were precipitated with 100% methanol, and each sample was resuspended in 2D cell lysis buffer (30 mM Tris-HCl, pH 8.8, 7 M urea, 2 M thiourea and 4% CHAPS). The mixture was sonicated at 4°C followed by shaking for 30 minutes at room temperature. The samples were then centrifuged for 30 minutes at 14,000 rpm and the supernatant was collected. Protein concentration was measured using the Bradford assay (Bio-Rad).

CyDye labeling

For each sample, 30μg of protein was mixed with CyDy2, Cy3 or Cy5 and kept in the dark on ice for 30 min. The labeling reaction was stopped by adding 10 mM lysine to each sample, and incubating in the dark on ice for an additional 15 min. The labeled samples were then mixed together. 2X 2-D Sample buffer (8 M urea, 4% CHAPS, 20 mg/ml DTT, 2% pharmalytes and trace amount of bromophenol blue), destreak solution (GE Healthcare), and rehydration buffer (7 M urea, 2 M thiourea, 4% CHAPS, 20 mg/ml DTT, 1% pharmalytes and trace amount of bromophenol blue) were added to a final volume of 260 ul. The samples were mixed well and spun down before loading onto the strip holder.

Isoelectric Focusing (IEF) and SDS-PAGE

After loading the labeled samples to pH 3-10 linear IPG strips (GE Healthcare), the IEF was run for 12 hours rehydration at 20°C, followed by 500 V for 1000 VHr, 1000 V for 2000 VHr, and 8000 V for 24000 VHr. Upon finishing the IEF, the IPG strips were incubated in freshly made equilibration buffer-1 (50 mM Tris-HCl, pH 8.8, containing 6 M urea, 30% glycerol, 2% SDS, trace amount of bromophenol blue and 10 mg/ml DTT) for 15 minutes with gentle shaking. Then the strips were rinsed in freshly made equilibration buffer-2 (50 mM Tris-HCl, pH 8.8, containing 6 M urea, 30% glycerol, 2% SDS, trace amount of bromophenol blue and 45 mg/ml Iodacetamide) for 10 minutes with gentle shaking. Next, the IPG strips were rinsed in SDS-gel running buffer before transferring into 12% SDS-gels (18 cm x 16 cm) followed by sealing with 0.5% Agarose (Bio-Rad) in SDS- polyacrylamide gel electrophoresis (SDS-PAGE) running buffer. The SDS-gels were run at 15°C until the dye front ran out of the gels.

Image scan and data analysis

Gel images were scanned immediately following the SDS-PAGE using Typhoon TRIO (Amersham BioSciences). The scanned images were then analyzed by Image Quant software Version 6.0 (Amersham BioSciences), followed by in-gel analysis using DeCyder software Version 6.0 (Amersham BioSciences). The DeCyder spot detection algorithm calculated ratio (volume of a spot from the secondary image/volume of the corresponding spot from the primary image), and a threshold of 1.5 fold change was set.

Protein identification by mass spectrometry

Spot picking and Trypsin digestion: The spots of interest were picked up by Ettan Spot Picker (Amersham BioSciences) based on the in-gel analysis and spot picking design by DeCyder software. The gel spots were washed a few times then digested in-gel with modified porcine trypsin protease (Trypsin Gold, Promega). The digested tryptic peptides were desalted by Zip-tip C18 (Millipore), and peptides were eluted from the Zip-tip with 0.5μl of Matrix solution (Agilent Technologies) and spotted on the MALDI plate (model ABI 01-192-6-AB). MALDI-TOF (MS) and TOF/TOF (tandem MS/MS) were performed on an ABI 4700 mass spectrometer (Applied Biosystems). MALDI-TOF mass spectra were acquired in reflection positive ion mode, averaging 4300 laser shots per spectrum. TOF/TOF tandem MS fragmentation spectra were acquired for each sample, averaging 4300 laser shots per fragmentation spectrum on each of the 10 most abundant ions present in each sample (excluding trypsin autolytic peptides and other known background ions). Both of the resulting peptide mass and the associated fragmentation spectra were submitted to GPS Explorer version 3.5 equipped with MASCOT search engine (Matrix Science) to search the database of National Center for Biotechnology Information non-redundant (NCBInr). The parameters were set at 800-4000 Da to create the “peak list.” Searches were performed without constraining protein molecular weight or isoelectric point, with variable carbamidomethylation of cysteine and oxidation of methionine residues, and with one

missed cleavage allowed in the search parameters. Mass tolerance was set at 0.3 Da and 100 ppm. Candidates with either protein score confidence interval (C.I.) % or Ion C.I.% greater than 95 were considered significant.

Network analysis

Ingenuity Pathway Analysis software (IPA) uses computational algorithms to identify and establish cellular networks that statistically fit the input protein list and expression values from experiments. Data sets containing gene names of the identified proteins and fold changes were overlaid onto a global molecular network developed from information contained in the database. Networks were then algorithmically generated based on their connectivity and a score was assigned. The score is used to rank networks according to how relevant they are to the molecules in the input dataset. Each network or pathway was arbitrarily set to have a maximum of 35 focus molecules. The significance of the association between the data set and the canonical pathways was determined by: (1) a ratio of the number of molecules from the data set that map to the pathway divided by the total number of molecules that map to the canonical pathway and (2) a P value calculated using Fischer's exact test.

Results

Physiological abnormalities following exposure to endocrine disruptors are accompanied by alterations at the protein level of individual cells. Our unpublished data showed a significant increase in PCB-induced vascularization with PCB153 concentrations of 10-100ng/ml while others have shown vascular tube formation at high micromolar concentrations (Tavolari, Bucci, Tomasi, & Guarnieri 2006). Therefore we further studied this endothelial cell phenotype by 2D-DIGE analysis of protein expression levels from human endothelial cells exposed 24h to either PCB153 or 17β-estradiol. PCB blood levels have been reported to reach approximately 1000ng/ml (~3μM) in occupationally exposed individuals (Wassermann et al. 1979). Based on known PCB blood levels from occupational exposure and our preliminary results; we chose a 10-fold lower PCB dose of 100ng/ml (~0.3μM) to expose endothelial cells. Our previous studies also showed endothelial cell proliferation and vascular tube formation at physiological doses of 17β-estradiol (Felty 2006;Felty and Porther 2008); therefore HMVEC were exposed to estradiol at 1ng/ml (~3.6nM).

Proteomic analyses of HMVEC exposed to PCB153 and estradiol

Two-dimensional difference in gel electrophoresis (2-D DIGE) analyses was performed on HMVEC cell lysate from 24h treatment with the vehicle, PCB153, or estradiol. Cell lysates were labeled with Cy2, Cy3 and Cy5; and the labeled samples were then combined for 2-D DIGE analysis. Three samples were simultaneously separated on a single 2D gel, using IEF in the first dimension using a linear pH 3-10 IPG strip, followed by a 12% SDS-PAGE in the second dimension. In Figure 1, cellular proteins from HMVEC were identified by 2D-DIGE. An average of 2200 spots was detected in each treatment group. HMVEC global protein expression analysis of PCB153 showed a 1.5% increase, 3.1% decrease, and similarity of 95.4% compared to control (Fig. 1A). Estradiol treatment showed a 6.9% increase, 4.3% decrease, and similarity of 88.8% in total protein levels when compared to control (Fig. 1B). In Figure 1C, estradiol treatment showed a 10.7% increase, 5.6% decrease, and 83.7% similarity when compared to PCB153 protein expression. ImageQuant software was used to generate overlay images which were subjected to DeCyder software analysis. The DeCyder spot detection algorithm calculated ratio (volume of a spot from the secondary image/volume of the corresponding spot from the primary image), and a threshold of 1.5 fold change was set. By using fold ≥ 1.5 as cutoff in the DeCyder analysis, a total of 96 well-resolved spots were selected. Those spots were circled and numbered in the large

overlay gel images (Fig. 2) and summarized in Table 1. From the 96 protein spots, 13 spots of interest were picked up by an Ettan Spot Picker based on the in-gel analysis and spot picking design by DeCyder software. Protein expression changes of the spots of interest were visualized by 3D imaging and integrated density (volume) was calculated for spots of interest (Fig. 3).

Identification of selected spots of interest

Protein identification was based on peptide fingerprint mass mapping and peptide fragmentation mapping. Tandem MS fragmentation spectra were acquired for each of the 10 most abundant ions present in each sample and submitted for the database search to identify proteins from the database of National Center for Biotechnology Information non-redundant (NCBInr). Candidates with either protein score confidence interval (C.I.) % or Ion C.I. % greater than 95 were considered significant. With these criteria, a total of 11 of the 13 selected spots of interest were successfully identified (Table 2). The identified proteins were classified with respect to their subcellular localization in order to get an overview of the effects of PCB153 and estradiol on the proteome of HMVEC. According to information collected by Ingenuity Pathways Analysis (IPA), all identified spots of interest were intracellular proteins distributed in the cytosol (64%) and nucleus (36%). Relative expression of the identified proteins indicated differentially expressed proteins between PCB153 and estradiol exposure (Table 3). The following proteins were up-regulated in estradiol treatment when compared to PCB153: filamin B, MX1 protein, cathepsin B, myosin regulatory light chain MRCL2, and ISG15 ubiquitin-like modifier. Proteins down-regulated by estradiol treatment when compared to PCB153: lamin B1, electron transfer flavoprotein chain A, vacuolar protein sorting 29, and cyclophilin A. Both experimental treatments showed that lamin A/C was down-regulated and far upstream element-binding protein was up-regulated.

Discussion

Estrogen produces both beneficial and adverse effects on cardiovascular health via mechanisms that remain unclear. Although estradiol–induced protein expression in endothelial cells has been studied, the question of whether estrogenic PCB-induced protein expression differs from the natural hormone 17β-estradiol has not been explored until now. This is the first report to our knowledge on the differential effects of the endocrine disruptor PCB153 and 17β-estradiol on the proteome of human microvascular endothelial cells. The HMVEC cell line is reported to express both estrogen receptors (ERα/β); and estradiol treatment was shown to increase phosphorylation of ERα (Klinge et al. 2005). Our previous studies have shown that physiological concentrations of estradiol (100pg-1ng/ml) induce the formation of reactive oxygen species (ROS) that are involved in signaling cell proliferation and vascularization (Felty 2006;Felty & Porther 2008). PCB153 has been shown to bind the ERα as well as induce vessel formation in endothelial cells (Tavolari, Bucci, Tomasi, & Guarnieri 2006). Discrepancies between the binding affinity of various estrogens to the ER and their growth potency both *in vitro* and *in vivo* have been reported (Bocchinfuso et al. 1999;DuMond, Jr. et al. 2001). Although selective ER modulators (SERMS) such as tamoxifen and antiestrogens such as ICI 182,780 prevent the growth of estrogen responsive cells, the contribution of other mechanisms cannot be ruled out as these chemicals also block metabolism and redox cycling of estrogen, and are free radical scavengers (Arteaga et al. 2003). Since the binding affinity of endocrine disruptors such as PCBs to the ER are relatively weak when compared to 17β-estradiol, we postulate that PCB153 activates redox signaling pathways that do not depend on the nuclear ER. Co-planar PCBs are reported to bind with a high affinity to the aryl hydrocarbon receptor (AhR) and induce AhR mediated gene expression of cytochrome P4501A1 (Hennig et al. 2002). This increase in CYP1A1

was implicated as a mechanism for ROS formation in PCB exposed endothelial cells reported by Hennig et al. However, non-coplanar PCBs like PCB153 are not good ligands for the AhR and their mechanisms of action are not completely understood. There is evidence for PCB153 mediated activation of NADPH oxidase which is a known source of cellular ROS that participates in redox signaling (Eum et al. 2009). This point may help explain why PCB153, a weak estrogen, induced endothelial tube formation comparable to estradiol (data unpublished). Since both PCB153 and estradiol increase ROS in endothelial cells, it is possible that PCB153 activates redox signaling pathways common to 17β-estradiol.

Using 2D-DIGE, a total of 96 well-resolved spots were selected that showed a fold change ≥1.5. A limitation of the 2D approach is that it will often miss small molecular weight and less abundant proteins, which may include important transcription regulatory molecules. Therefore spots of interest were not chosen entirely on dramatic fold differences between treatments. From the 96 spots, we selected 13 spots for further protein identification analysis. The analyses identified 11 of the 13 spots of interest with high confidence protein score C.I. that was greater than 99% (Table 2). Of the identified proteins, Lamin A/C (LMNA) and far upstream element-binding protein (FUBP1) were of particular interest because they were regulated similarly by both PCB153 and estradiol treatment (Table 3). A-type lamins play important roles in the control of gene expression in the nucleus. For example, lamin A/C suppresses transcription factor AP-1 function through direct interaction with c-fos (Ivorra et al. 2006). Mitogen-induced ERK1/2-mediated phosphorylation of c-fos releases it from the inhibitory interaction with lamin A/C before de novo synthesis of c-fos, thus allowing a rapid induction of AP-1 activity (Gonzalez et al. 2008). We have previously shown that estrogen-induced ROS activate the binding of the AP-1 which is a known redox sensitive transcription factor (Felty et al. 2005b). Since both PCB153 and estradiol treatment down-regulated lamin A/C, we postulate that this decrease in lamin A/C will lead to an increase in free or unbound nuclear c-fos. It is this unbound c-fos that will result in an increase in AP-1 activity allowing for the expression of cell cycle genes contributing to cell growth. Interestingly, FUBP1 is another protein involved in the regulation of gene transcription. FUBP1 is reported to bind an upstream element of the c-myc promoter and regulates the c-myc mRNA level (Bazar et al. 1995). In estrogen dependent MCF-7 cells, FUBP1 was recently identified to be differentially expressed after PCB153 and atrazine exposure (Lasserre et al. 2009). Regulation of the expression levels of FUBP1 is of particular significance in vascular lesions formation due to its ability to control the level of c-myc in the cell. Although c-myc has classically been considered to be involved in cancer, advanced stages of vascular lesions are characterized by a local increase in tissue mass which has brought attention to potential c-myc involvement in CVD. For instance, c-myc is implicated in both endothelial dysfunction and atherogenesis (de et al. 2003). In vascular cells, c-myc was shown to be activated by ROS (Rao and Berk 1992). Based on these findings, we postulate that PCB153 and estradiol increase FUBP1 which in turn controls the level of c-myc in a redox sensitive pathway. Since c-myc is known to regulate genes that are required for cell growth, PCB153 and estradiol treatments may elicit their effects on cell proliferation and vascular tube formation via FUBP1.

Proteins that were up-regulated by estradiol treatment when compared to PCB153 included myosin regulatory light chain MRCL2 (MYL12B), filamin B (FLNB), cathepsin B (CTSB), MX1 protein (MX1), and ISG15 ubiquitin-like modifier (ISG15). Estradiol treatment showed a fold increase ≥1.5 for myosin regulatory light chain MRCL2 isoform A. Phosphorylation of the regulatory light chain of myosin II such as MRLC2 is a primary means of activating myosin II and is known to be crucial for the execution of cell division (Iwasaki et al. 2001). An increase in MRLC2 protein may be associated with supporting estrogen-induced endothelial cell proliferation that we and others have reported (Felty

2006). Estradiol exposed HMVEC also showed a 2.3 fold increase in the level of filamin B; a family of actin binding proteins involved in connecting the plasma membrane and its integral proteins with the actin cytoskeleton (Calderwood et al. 2000). Disruption of filamin B is reported to inhibit VEGF-induced capillary tube formation in 3D collagen gels and inhibition of cell migration (Del Valle-Perez et al. 2010). Since estrogen is known to increase VEGF and tube formation by endothelial cells, the observed increase in filamin B is expected. Cathepsin B is an enzymatic protein belonging to a group of cysteine proteases. Localization of proteases to the surface of endothelial cells and remodeling of the extracellular matrix are essential to endothelial cell tube formation. During in vitro capillary tube formation, active cathepsin B has been shown to increase in caveolar fractions (Cavallo-Medved et al. 2009). Thus, cathepsin B could play a role in signaling vascularization by estradiol. Myxovirus resistance 1 protein (MX1) is similar to mouse protein that protects against flu infection by influenza A virus and rhabdovirus (Pavlovic and Staeheli 1991). Interferon gamma exposure is reported to induce MX1 gene expression and the MX1 protein in human uterine microvascular endothelial cells, but whether MX1 expression is due to an estrogen-induced inflammatory response or ROS is not known (Kitaya et al. 2007). ISG15 is a ubiquitin-like modifier modifier(Haas et al. 1987). Similar to ubiquitin, ISG15 becomes conjugated to a variety of proteins (ISGlyation) when cells are treated with type I interferon or lipopolysaccharide (Loeb and Haas 1992); a process which is similar to protein ubiquitylation, however, ISG15 conjugation does not increase the degradation of ISGylated proteins (Malakhov et al. 2003). Cysteine residues of ISG15 have been shown to be modified by nitric oxide (NO) (Okumura et al. 2008). Furthermore, it was reported that nitrosylation of ISG15 decreased the dimerization of ISG15 which in turn increased the availability of free ISG15 to be used for ISGylation. Key regulators of signal transduction have been identified to be conjugated with ISG15: phospholipase Cγ1; kinases Jak1 and ERK1; and the transcription factor Stat1 (Malakhov, Kim, Malakhova, Jacobs, Borden, & Zhang 2003). Although many targets of ISGylation have now been identified, the consequences of modification by ISG15 are in most cases unknown. It is generally believed that the primary target of estrogens in the cardiovascular system is endothelial nitric oxide synthase (eNOS). Estrogen is known to mediate the production of NO and similarly PCBs have also been shown to increase eNOS phosphorylation and NO production in human vascular endothelial cells (Lim et al. 2007). Although its role in estrogen-induced vascularization is not known, ISG15 may potentially be regulated by reactive nitrogen species from our experimental treatments.

Proteins down-regulated by estradiol treatment when compared to PCB153 included lamin B1 (LMNB1), cyclophilin A (CyPA), electron transfer flavoprotein A (ETFA), and vacuolar protein sorting 29 (VPS29). PCB153 treatment increased lamin B1 1.85-fold when compared to control. Lamin B1 at the nuclear lamina was shown to sequester octamer transcription factor 1 (Oct-1) (Malhas et al. 2009). Oct-1 has been reported to be a repressor of genes important for the cellular response to oxidative stress (Tantin et al. 2005). Disrupting the interactions between lamin B1 and Oct-1 resulted in the overall down-regulation of oxidative stress response genes. Based on these reports, the increase of lamin B1 may help HMVEC with excess ROS formation from PCB153 exposure. Sequestering Oct-1 would allow for the activation of oxidative stress response genes ultimately leading to a reduction of oxidant levels in the cell. Cyclophilin A (CyPA) is a cytosolic protein possessing peptidyl-prolyl isomerase (PPIase) and chaperone activities. CypA is alleged to contribute to the correct folding of misfolded proteins that have accumulated due to stress. CyPA was shown to be highly expressed in atherosclerotic plaques from the ApoE–/– mouse. Endothelial cells exposed to CyPA show increased in cell proliferation, migration, invasive capacity, and tubulogenesis (Kim et al. 2004). CyPA was shown to be secreted by VSMCs in response to oxidative stress and mediated ERK1/2 activation and VSMC growth by ROS (Jin et al. 2000). Evidence for CyPA as a secreted redox-sensitive mediator and its

reported effects in vascular cells suggest an important role for CyPA in the pathogenesis of vascular diseases. CyPA was reported to significantly increase cell proliferation of human lung endothelial cells, however, it is not known whether pulmonary vascular lesions show an increase in CyPA (Yang et al. 2005). Electron transfer flavoproteins function as electron shuttles between primary flavoprotein dehydrogenases involved in mitochondrial fatty acid and amino acid catabolism and the membrane-bound electron transfer flavoprotein ubiquinone oxidoreductase (Roberts et al. 1996). We have shown that estrogen-induced mitochondrial ROS signal DNA synthesis in endothelial cells (Felty et al. 2005a;Felty 2006), it is not clear how down-regulation of ETF would affect ROS production in HMVEC. Vacuolar protein sorting 29 is a component of a large multimeric complex, termed the retromer complex, which is involved in retrograde transport of proteins from endosomes to the trans-Golgi network (Wang et al. 2005).

The identified proteins regulated by PCB153 and estradiol were analyzed using IPA software to identify significant networks. The results provide information on how the dataset overlaps molecules associated with various diseases and cellular functions. The number one ranked network (score=30, focus molecules = 11) (Fig. 4A) was associated with Cardiovascular System Development and Function, Organism Development, and Drug Metabolism. Transforming growth factor β-1 (TGFB1) and the transcription factor c-myc play central roles in the identified network. The top biological functions of networks associated with the identified proteins are summarized in Fig. 4B. Interestingly, we have recently shown both PCB153 and estradiol treatment to significantly up-regulate ≥2-fold TGFB2 mRNA expression in HMVEC (Felty, Q et al. in press). According to the KEGG database TGFB2 functions through the same receptor signaling system as TGFB1. Further supporting the biological significance of TGFB1 network identified by IPA analysis in PCB153 and estradiol exposed HMVEC.

Although estrogen-induced protein expression has been studied in endothelial cells, there is a lack of knowledge about how the protein expression profile differs from exposure to endocrine disruptors. Several epidemiological studies have shown a link between PCB exposure and increased risk of CVD (Goncharov et al. 2008;Gustavsson and Hogstedt 1997;Hay and Tarrel 1997;Sergeev and Carpenter 2005;Tokunaga and Kataoka 2003). Considering the recent studies that question the previously reported cardio-protective effects of estrogens, there is a growing concern that endocrine disruptors such as PCB153 may increase the risk for PAH by inducing the formation of pulmonary vascular lesions. Growing evidence implicates the overproduction of ROS such as hydrogen peroxide (H_2O_2), superoxide anion (O_2•-), and peroxynitrite (ONOO-) in the development of CVD. Thus, identification of redox signaling pathways that mediate vascularization may add to the knowledge base of how endocrine disruptors affect the vascular wall. Advanced stages of vascular lesion formation are characterized by a local increase in tissue mass. This increase in tissue mass can be attributed to oxidation-sensitive modification of cell cycle-related events, including cellular proliferation. While our findings do not reveal any mechanisms involved in PCB153 induced vascularization, the identified network does provide a potential target pathway for further mechanistic studies of these relationships.

Acknowledgments

This work was supported in part by grants from NIH SC3GM084827 (Felty, Q.) and the Florida Biomedical Research Bankhead-Coley Award 09BN-06 (Felty, Q.).

References

Arteaga E, Villaseca P, Bianchi M, Rojas A, Marshall G. Raloxifene is a better antioxidant of low-density lipoprotein than estradiol or tamoxifen in postmenopausal women in vitro. Menopause. 2003; 10(2):142–146. available from: PM:12627039. [PubMed: 12627039]

Bazar L, Meighen D, Harris V, Duncan R, Levens D, Avigan M. Targeted melting and binding of a DNA regulatory element by a transactivator of c-myc. J.Biol.Chem. 1995; 270(14):8241–8248. available from: PM:7713931. [PubMed: 7713931]

Bitman J, Cecil HC. Estrogenic activity of DDT analogs and polychlorinated biphenyls. J.Agric.Food Chem. 1970; 18(6):1108–1112. available from: PM:5483049. [PubMed: 5483049]

Bocchinfuso WP, Hively WP, Couse JF, Varmus HE, Korach KS. A mouse mammary tumor virus-Wnt-1 transgene induces mammary gland hyperplasia and tumorigenesis in mice lacking estrogen receptor-alpha. Cancer Res. 1999; 59(8):1869–1876. available from: PM:10213494. [PubMed: 10213494]

Calderwood DA, Shattil SJ, Ginsberg MH. Integrins and actin filaments: reciprocal regulation of cell adhesion and signaling. J.Biol.Chem. 2000; 275(30):22607–22610. available from: PM:10801899. [PubMed: 10801899]

Cavallo-Medved D, Rudy D, Blum G, Bogyo M, Caglic D, Sloane BF. Live-cell imaging demonstrates extracellular matrix degradation in association with active cathepsin B in caveolae of endothelial cells during tube formation. Exp.Cell Res. 2009; 315(7):1234–1246. available from: PM:19331819. [PubMed: 19331819]

Cid MC, Schnaper HW, Kleinman HK. Estrogens and the vascular endothelium. Ann.N.Y.Acad.Sci. 2002; 966:143–157. available from: PM:12114268. [PubMed: 12114268]

Davey JC, Bodwell JE, Gosse JA, Hamilton JW. Arsenic as an endocrine disruptor: effects of arsenic on estrogen receptor-mediated gene expression in vivo and in cell culture. Toxicol.Sci. 2007; 98(1): 75–86. available from: PM:17283378. [PubMed: 17283378]

de NF, Sica V, Herrmann J, Condorelli G, Chade AR, Tajana G, Lerman A, Lerman LO, Napoli C. c-Myc oncoprotein: cell cycle-related events and new therapeutic challenges in cancer and cardiovascular diseases. Cell Cycle. 2003; 2(4):325–328. available from: PM:12851483. [PubMed: 12851483]

Del Valle-Perez B, Martinez VG, Lacasa-Salavert C, Figueras A, Shapiro SS, Takafuta T, Casanovas O, Capella G, Ventura F, Vinals F. Filamin B plays a key role in VEGF-induced endothelial cell motility through its interaction with Rac-1 and Vav-2. J.Biol.Chem. 2010 available from: PM: 20110358.

DuMond JW Jr. Singh KP, Roy D. Regulation of the growth of mouse Leydig cells by the inactive stereoisomer, 17alpha-estradiol: Lack of correlation between the elevated expression of ERalpha and difference in sensitivity to estradiol isomers. Oncol.Rep. 2001; 8(4):899–902. available from: PM:11410806. [PubMed: 11410806]

Eum SY, Andras I, Hennig B, Toborek M. NADPH oxidase and lipid raft-associated redox signaling are required for PCB153-induced upregulation of cell adhesion molecules in human brain endothelial cells. Toxicol.Appl.Pharmacol. 2009; 240(2):299–305. available from: PM:19632255. [PubMed: 19632255]

Felty Q. Estrogen-induced DNA synthesis in vascular endothelial cells is mediated by ROS signaling. BMC.Cardiovasc.Disord. 2006; 6:16. available from: PM:16608521. [PubMed: 16608521]

Felty Q, Porther N. Estrogen-induced redox sensitive Id3 signaling controls the growth of vascular cells. Atherosclerosis. 2008; 198(1):12–21. available from: PM:18281048. [PubMed: 18281048]

Felty Q, Singh KP, Roy D. Estrogen-induced G(1)/S transition of G(0)-arrested estrogen-dependent breast cancer cells is regulated by mitochondrial oxidant signaling. Oncogene. 2005a available from: PM:15897899.

Felty Q, Xiong WC, Sun D, Sarkar S, Singh KP, Parkash J, Roy D. Estrogen-induced mitochondrial reactive oxygen species as signal-transducing messengers. Biochemistry. 2005b; 44(18):6900–6909. available from: PM:15865435. [PubMed: 15865435]

Goncharov A, Haase RF, Santiago-Rivera A, Morse G, McCaffrey RJ, Rej R, Carpenter DO. High serum PCBs are associated with elevation of serum lipids and cardiovascular disease in a Native

American population. Environ Res. 2008; 106(2):226–239. available from: PM:18054906. [PubMed: 18054906]

Gonzalez JM, Navarro-Puche A, Casar B, Crespo P, Andres V. Fast regulation of AP-1 activity through interaction of lamin A/C, ERK1/2, and c-Fos at the nuclear envelope. J.Cell Biol. 2008; 183(4):653–666. available from: PM:19015316. [PubMed: 19015316]

Gustavsson P, Hogstedt C. A cohort study of Swedish capacitor manufacturing workers exposed to polychlorinated biphenyls (PCBs). Am J.Ind.Med. 1997; 32(3):234–239. available from: PM: 9219652. [PubMed: 9219652]

Haas AL, Ahrens P, Bright PM, Ankel H. Interferon induces a 15-kilodalton protein exhibiting marked homology to ubiquitin. J.Biol.Chem. 1987; 262(23):11315–11323. available from: PM:2440890. [PubMed: 2440890]

Hay A, Tarrel J. Mortality of power workers exposed to phenoxy herbicides and polychlorinated biphenyls in waste transformer oil. Ann.N.Y.Acad.Sci. 1997; 837:138–156. available from: PM: 9472337. [PubMed: 9472337]

Hennig B, Hammock BD, Slim R, Toborek M, Saraswathi V, Robertson LW. PCB-induced oxidative stress in endothelial cells: modulation by nutrients. Int.J.Hyg.Environ Health. 2002; 205(1-2):95–102. available from: PM:12018021. [PubMed: 12018021]

Hyduk A, Croft JB, Ayala C, Zheng K, Zheng ZJ, Mensah GA. Pulmonary hypertension surveillance--United States, 1980-2002. MMWR Surveill Summ. 2005; 54(5):1–28. available from: PM: 16280974. [PubMed: 16280974]

Irey NS, Norris HJ. Intimal vascular lesions associated with female reproductive steroids. Arch.Pathol. 1973; 96(4):227–234. available from: PM:4743889. [PubMed: 4743889]

Ivorra C, Kubicek M, Gonzalez JM, Sanz-Gonzalez SM, Alvarez-Barrientos A, O'Connor JE, Burke B, Andres V. A mechanism of AP-1 suppression through interaction of c-Fos with lamin A/C. Genes Dev. 2006; 20(3):307–320. available from: PM:16452503. [PubMed: 16452503]

Iwasaki T, Murata-Hori M, Ishitobi S, Hosoya H. Diphosphorylated MRLC is required for organization of stress fibers in interphase cells and the contractile ring in dividing cells. Cell Struct.Funct. 2001; 26(6):677–683. available from: PM:11942626. [PubMed: 11942626]

Jin ZG, Melaragno MG, Liao DF, Yan C, Haendeler J, Suh YA, Lambeth JD, Berk BC. Cyclophilin A is a secreted growth factor induced by oxidative stress. Circ.Res. 2000; 87(9):789–796. available from: PM:11055983. [PubMed: 11055983]

Kim SH, Lessner SM, Sakurai Y, Galis ZS. Cyclophilin A as a novel biphasic mediator of endothelial activation and dysfunction. Am.J.Pathol. 2004; 164(5):1567–1574. available from: PM:15111303. [PubMed: 15111303]

Kitaya K, Yasuo T, Yamaguchi T, Fushiki S, Honjo H. Genes regulated by interferon-gamma in human uterine microvascular endothelial cells. Int.J.Mol.Med. 2007; 20(5):689–697. available from: PM:17912462. [PubMed: 17912462]

Kleiger RE, Boxer M, Ingham RE, Harrison DC. Pulmonary hypertension in patients using oral contraceptives. A report of six cases. Chest. 1976; 69(2):143–147. available from: PM:1248265. [PubMed: 1248265]

Klinge CM, Blankenship KA, Risinger KE, Bhatnagar S, Noisin EL, Sumanasekera WK, Zhao L, Brey DM, Keynton RS. Resveratrol and estradiol rapidly activate MAPK signaling through estrogen receptors alpha and beta in endothelial cells. J.Biol.Chem. 2005; 280(9):7460–7468. available from: PM:15615701. [PubMed: 15615701]

Lasserre JP, Fack F, Revets D, Planchon S, Renaut J, Hoffmann L, Gutleb AC, Muller CP, Bohn T. Effects of the endocrine disruptors atrazine and PCB 153 on the protein expression of MCF-7 human cells. J.Proteome.Res. 2009; 8(12):5485–5496. available from: PM:19778091. [PubMed: 19778091]

Lim EJ, Smart EJ, Toborek M, Hennig B. The role of caveolin-1 in PCB77-induced eNOS phosphorylation in human-derived endothelial cells. Am J.Physiol Heart Circ.Physiol. 2007; 293(6):H3340–H3347. available from: PM:17933968. [PubMed: 17933968]

Loeb KR, Haas AL. The interferon-inducible 15-kDa ubiquitin homolog conjugates to intracellular proteins. J.Biol.Chem. 1992; 267(11):7806–7813. available from: PM:1373138. [PubMed: 1373138]

Malakhov MP, Kim KI, Malakhova OA, Jacobs BS, Borden EC, Zhang DE. High-throughput immunoblotting. Ubiquitiin-like protein ISG15 modifies key regulators of signal transduction. J.Biol.Chem. 2003; 278(19):16608–16613. available from: PM:12582176. [PubMed: 12582176]

Malhas AN, Lee CF, Vaux DJ. Lamin B1 controls oxidative stress responses via Oct-1. J.Cell Biol. 2009; 184(1):45–55. available from: PM:19139261. [PubMed: 19139261]

Meek MD, Finch GL. Diluted mainstream cigarette smoke condensates activate estrogen receptor and aryl hydrocarbon receptor-mediated gene transcription. Environ.Res. 1999; 80(1):9–17. available from: PM:9931222. [PubMed: 9931222]

Newman JH, Fanburg BL, Archer SL, Badesch DB, Barst RJ, Garcia JG, Kao PN, Knowles JA, Loyd JE, McGoon MD, Morse JH, Nichols WC, Rabinovitch M, Rodman DM, Stevens T, Tuder RM, Voelkel NF, Gail DB. Pulmonary arterial hypertension: future directions: report of a National Heart, Lung and Blood Institute/Office of Rare Diseases workshop. Circulation. 2004; 109(24): 2947–2952. available from: PM:15210611. [PubMed: 15210611]

Okumura F, Lenschow DJ, Zhang DE. Nitrosylation of ISG15 prevents the disulfide bond-mediated dimerization of ISG15 and contributes to effective ISGylation. J.Biol.Chem. 2008; 283(36): 24484–24488. available from: PM:18606809. [PubMed: 18606809]

Pavlovic J, Staeheli P. The antiviral potentials of Mx proteins. J.Interferon Res. 1991; 11(4):215–219. available from: PM:1919077. [PubMed: 1919077]

Rao GN, Berk BC. Active oxygen species stimulate vascular smooth muscle cell growth and proto-oncogene expression. Circ.Res. 1992; 70(3):593–599. available from: PM:1371430. [PubMed: 1371430]

Roberts DL, Frerman FE, Kim JJ. Three-dimensional structure of human electron transfer flavoprotein to 2.1-A resolution. Proc.Natl.Acad.Sci.U.S.A. 1996; 93(25):14355–14360. available from: PM: 8962055. [PubMed: 8962055]

Rossouw JE. Coronary heart disease in menopausal women: implications of primary and secondary prevention trials of hormones. Maturitas. 2005; 51(1):51–63. available from: PM:15883110. [PubMed: 15883110]

Sakao S, Tatsumi K, Voelkel NF. Endothelial cells and pulmonary arterial hypertension: apoptosis, proliferation, interaction and transdifferentiation. Respir.Res. 2009; 10:95. available from: PM: 19825167. [PubMed: 19825167]

Sergeev AV, Carpenter DO. Hospitalization rates for coronary heart disease in relation to residence near areas contaminated with persistent organic pollutants and other pollutants. Environ Health Perspect. 2005; 113(6):756–761. available from: PM:15929900. [PubMed: 15929900]

Tantin D, Schild-Poulter C, Wang V, Hache RJ, Sharp PA. The octamer binding transcription factor Oct-1 is a stress sensor. Cancer Res. 2005; 65(23):10750–10758. available from: PM:16322220. [PubMed: 16322220]

Tavolari S, Bucci L, Tomasi V, Guarnieri T. Selected polychlorobiphenyls congeners bind to estrogen receptor alpha in human umbilical vascular endothelial (HUVE) cells modulating angiogenesis. Toxicology. 2006; 218(1):67–74. available from: PM:16293362. [PubMed: 16293362]

Tokunaga S, Kataoka K. [A longitudinal analysis on the association of serum lipids and lipoproteins concentrations with blood polychlorinated biphenyls level in chronic “Yusho” patients]. Fukuoka Igaku Zasshi. 2003; 94(5):110–117. available from: PM:12872711. [PubMed: 12872711]

Venetsanakos E, Mirza A, Fanton C, Romanov SR, Tlsty T, McMahon M. Induction of tubulogenesis in telomerase-immortalized human microvascular endothelial cells by glioblastoma cells. Exp.Cell Res. 2002; 273(1):21–33. available from: PM:11795943. [PubMed: 11795943]

Wang D, Guo M, Liang Z, Fan J, Zhu Z, Zang J, Zhu Z, Li X, Teng M, Niu L, Dong Y, Liu P. Crystal structure of human vacuolar protein sorting protein 29 reveals a phosphodiesterase/nuclease-like fold and two protein-protein interaction sites. J.Biol.Chem. 2005; 280(24):22962–22967. available from: PM:15788412. [PubMed: 15788412]

Wassermann M, Wassermann D, Cucos S, Miller HJ. World PCBs map: storage and effects in man and his biologic environment in the 1970s. Ann.N.Y.Acad.Sci. 1979; 320:69–124. available from: PM:110205. [PubMed: 110205]

Yang H, Li M, Chai H, Yan S, Lin P, Lumsden AB, Yao Q, Chen C. Effects of cyclophilin A on cell proliferation and gene expressions in human vascular smooth muscle cells and endothelial cells. J.Surg.Res. 2005; 123(2):312–319. available from: PM:15680395. [PubMed: 15680395]

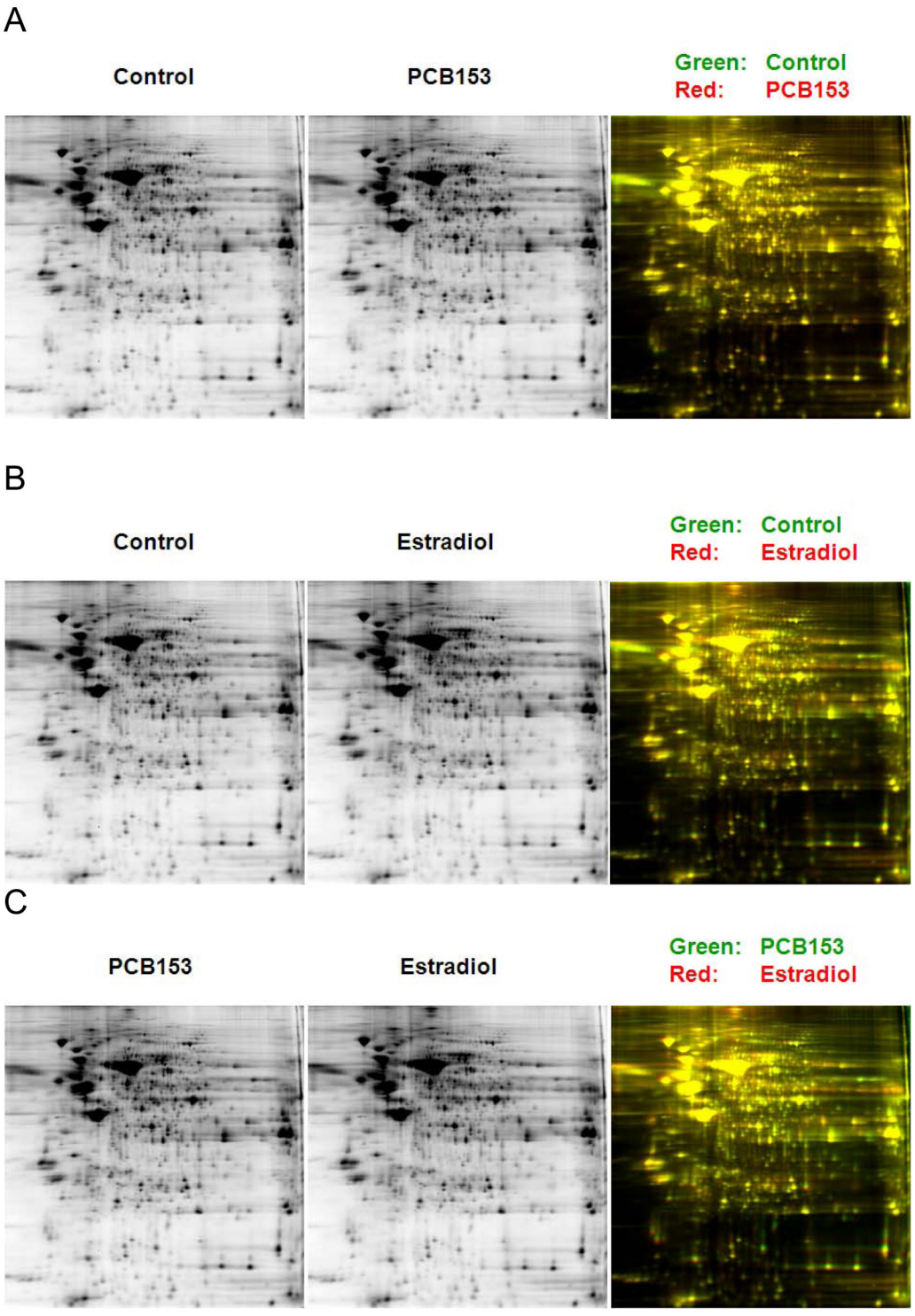

Figure 1.

Cellular proteins from cultured human microvascular endothelial cells (HMVEC) identified by 2D-DIGE. HMVECs were treated with PCB153 (100ng/ml) or 17β-estradiol (1ng/ml) for 24h. Each sample was labeled with CyDye DIGE fluors. Three samples were simultaneously separated on a single 2D gel, using IEF in the first dimension using a linear pH 3-10 IPG strip, followed by a 12% SDS-PAGE in the second dimension. After electrophoresis, the gel

was scanned using a Typhoon image scanner. ImageQuant software was used to generate the image presentation data including the single and overlay images: (A) Control (green) and PCB153 (red); (B) Control (green) and Estradiol (red); and (C) PCB153 (green) and Estradiol (red). Control treatment was vehicle DMSO (0.1%). Representative gel images are shown.

A

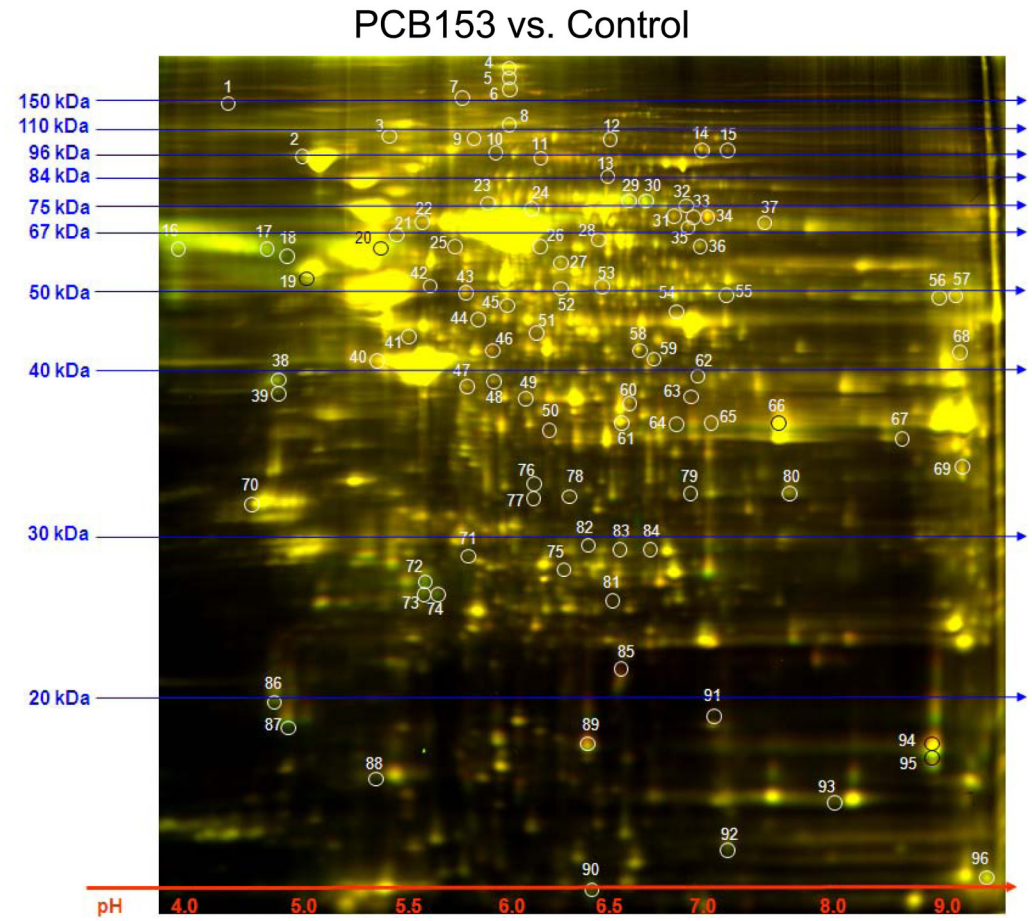

B

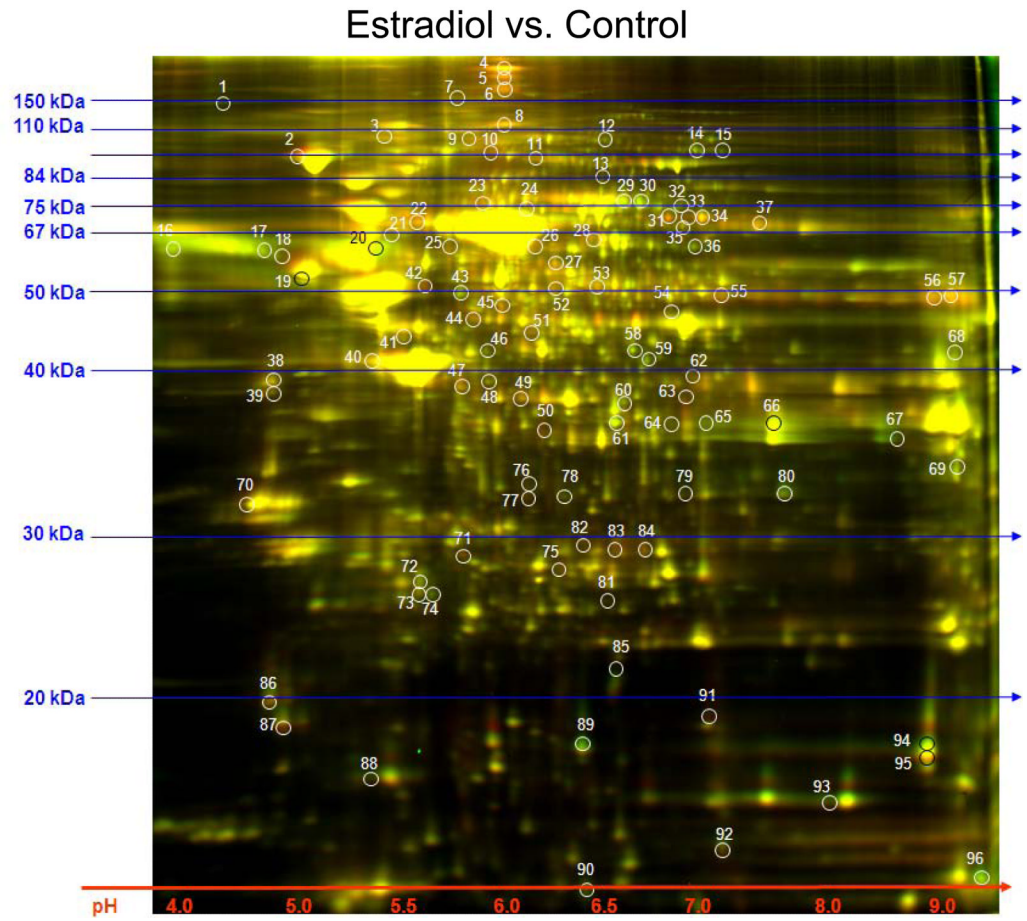

C

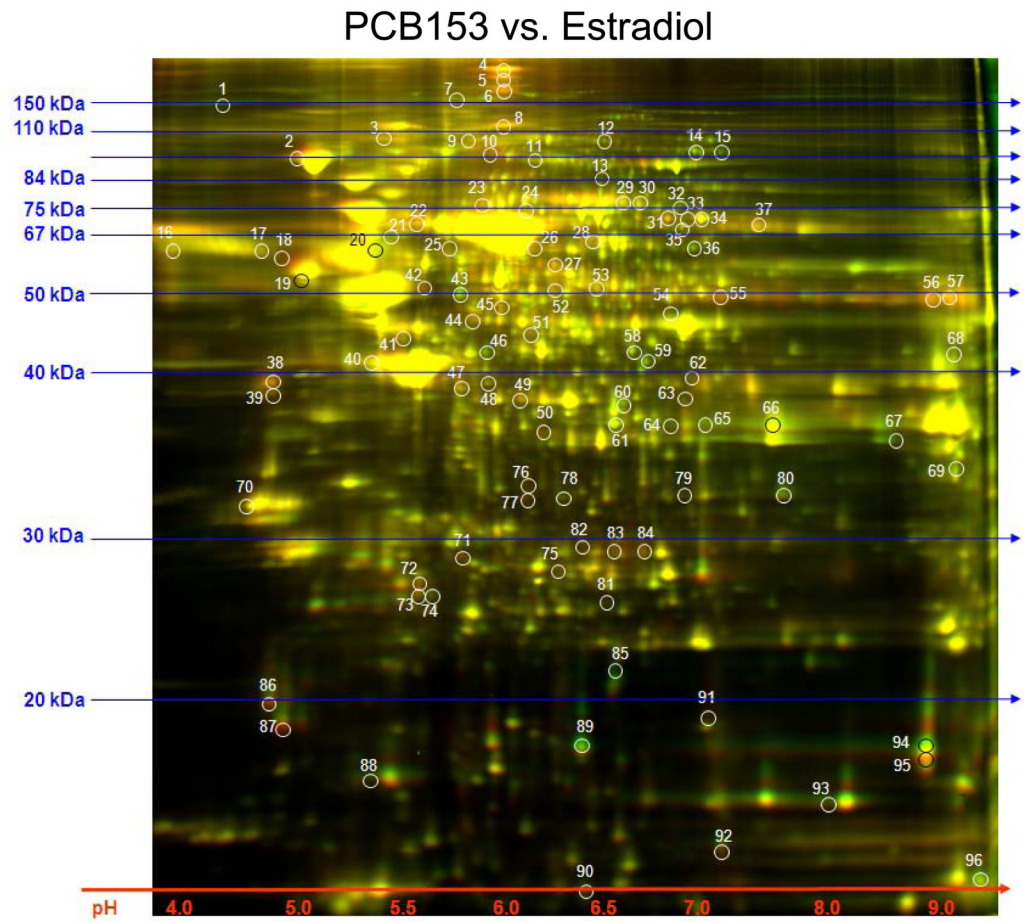

Figure 2.

Enlarged gel image from overlay of 2 samples. ImageQuant software was used to generate overlay images which were subjected to DeCyder software analysis Version 6.0. The DeCyder spot detection algorithm calculated ratio (volume of a spot from the secondary image/volume of the corresponding spot from the primary image), and a threshold of 1.5 fold change was set. By using fold ≥ 1.5 as cutoff in the DeCyder analysis, a total of 96 well-resolved spots were selected. Those spots were circled and numbered in the large overlay gel images. (A) Gel image from overlay of Control (Green) and PCB153 (Red). (B) Gel image from overlay of Control (Green) and Estradiol (Red). (C) Gel image from overlay of PCB153 (Green) and Estradiol (Red).

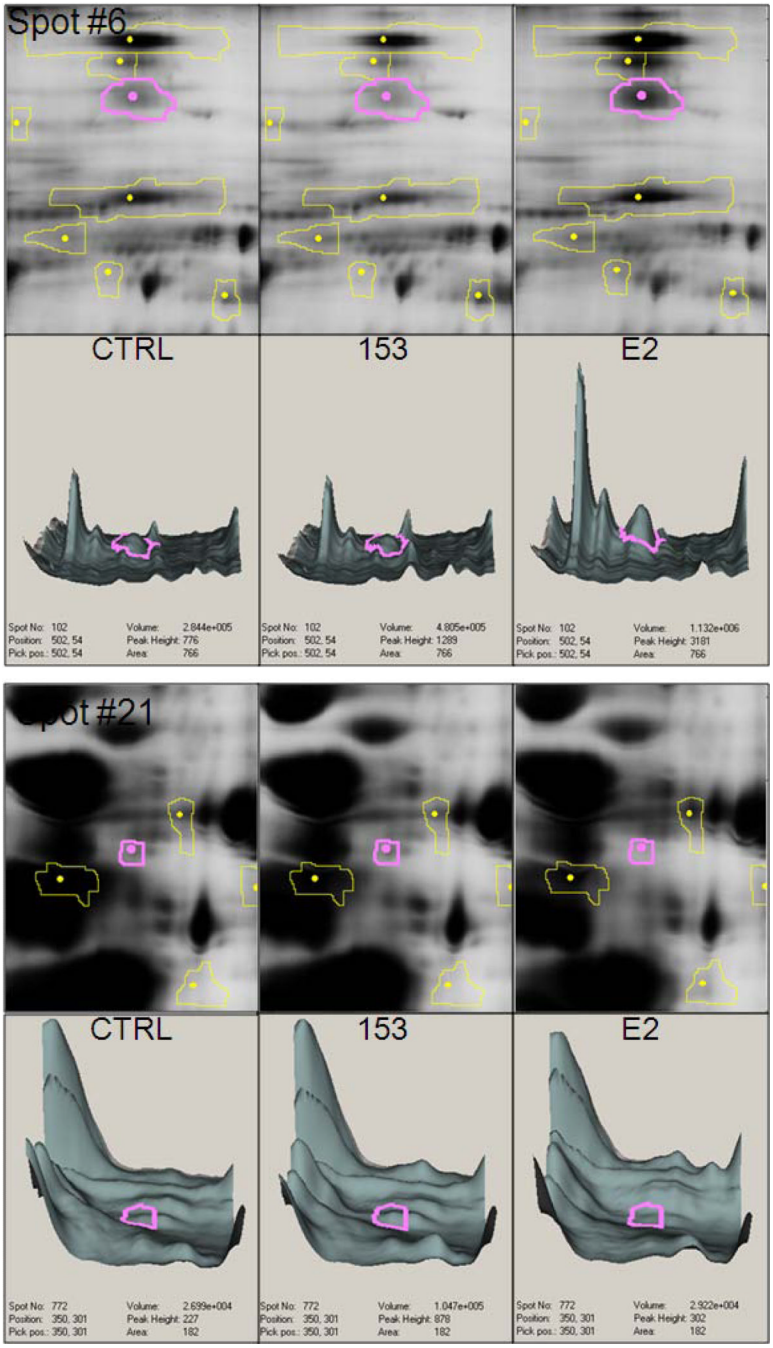

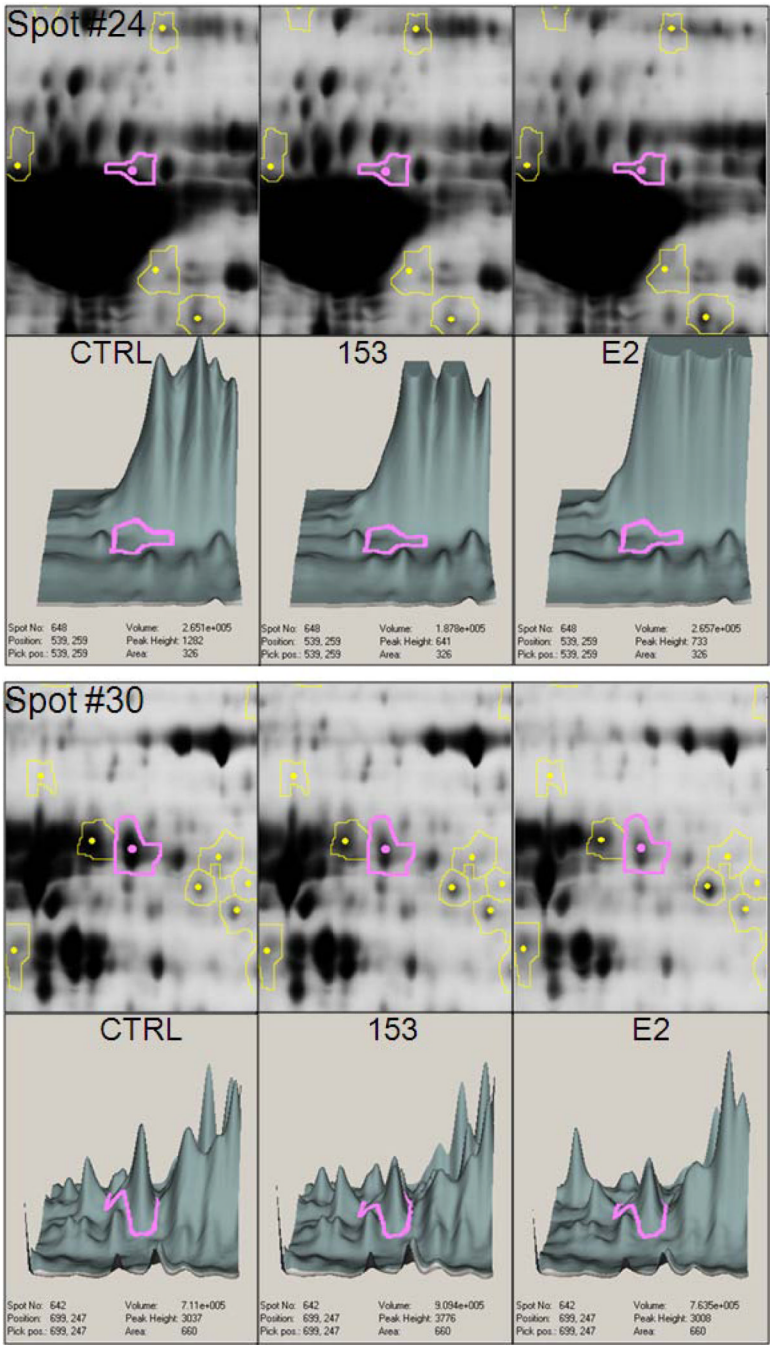

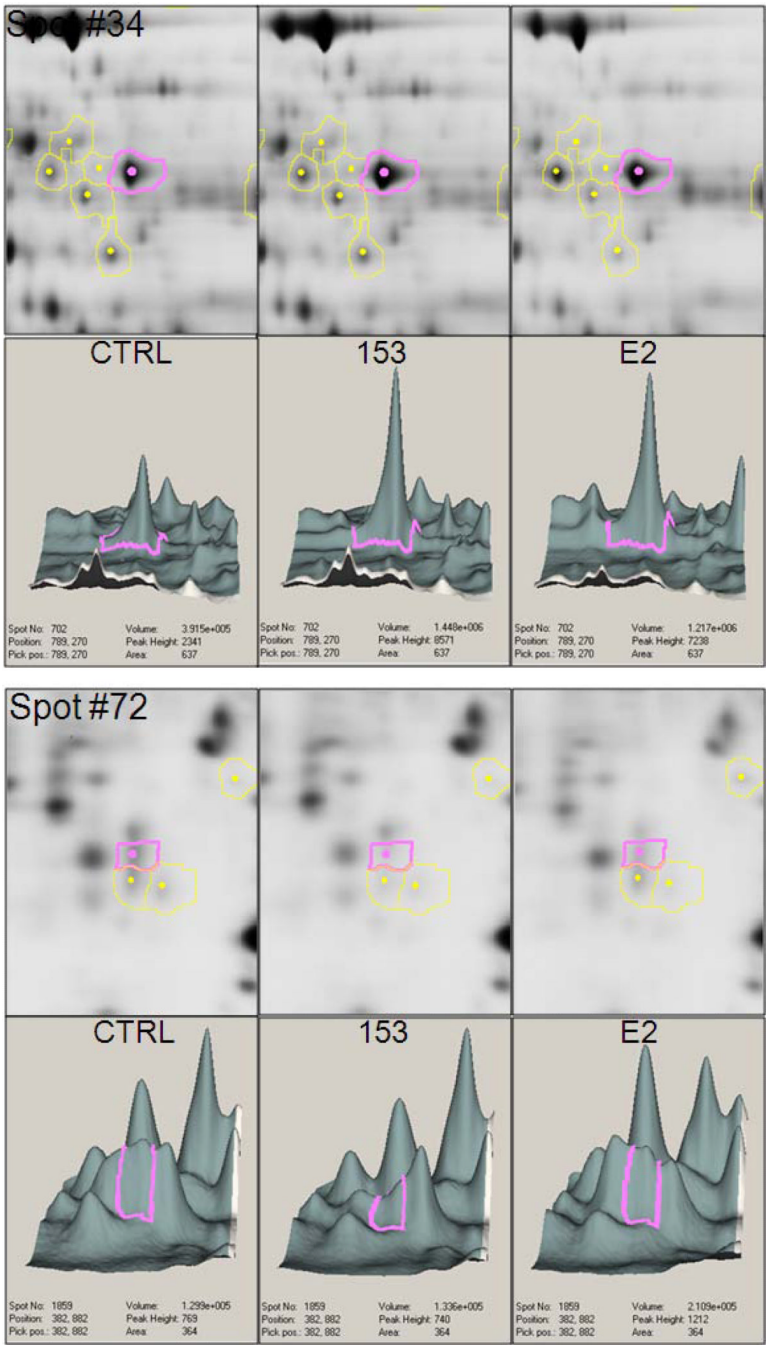

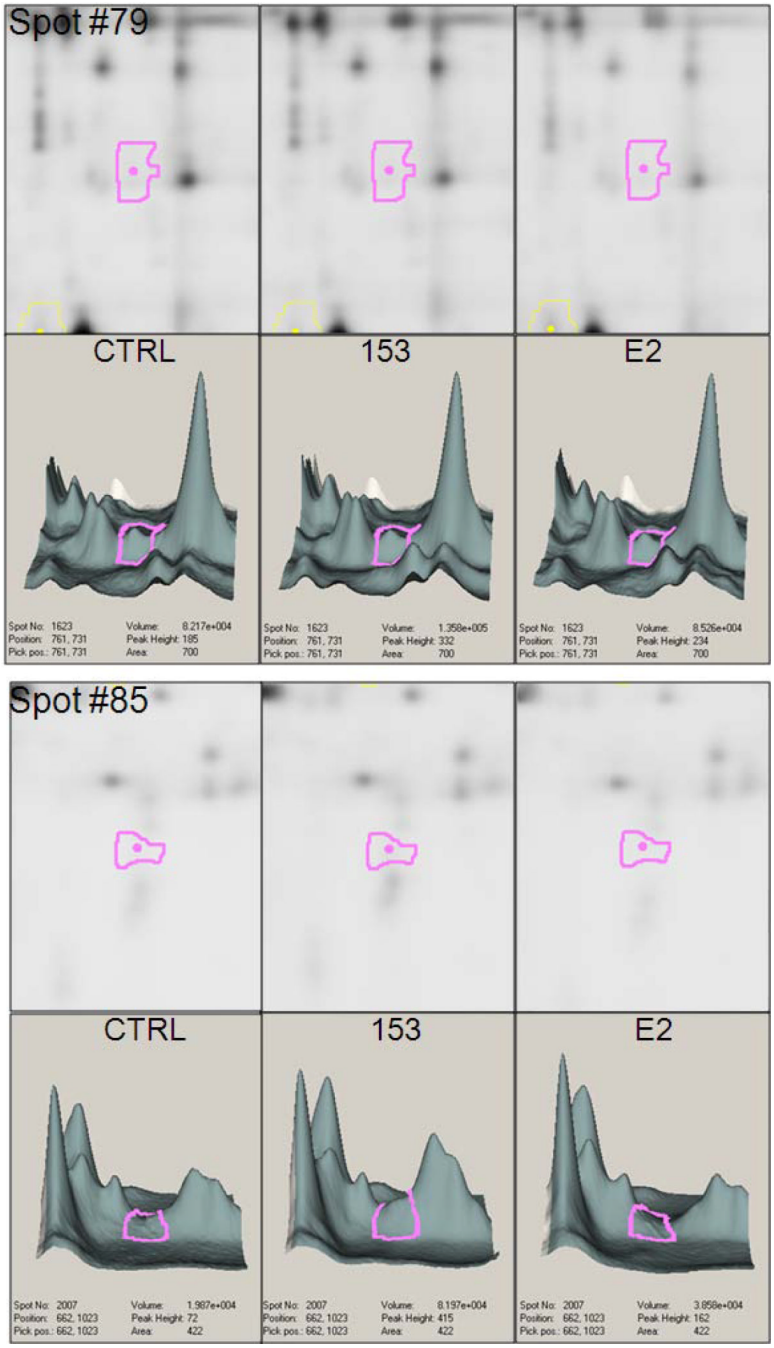

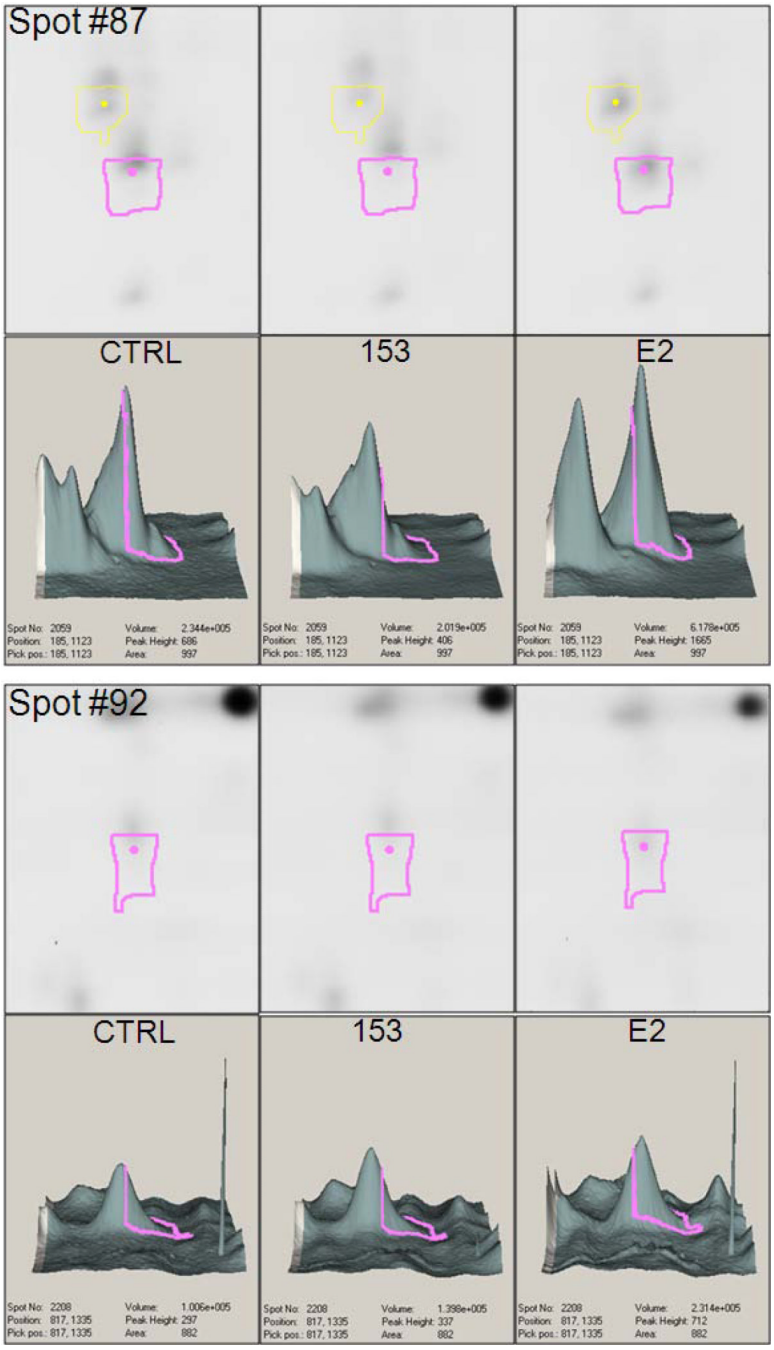

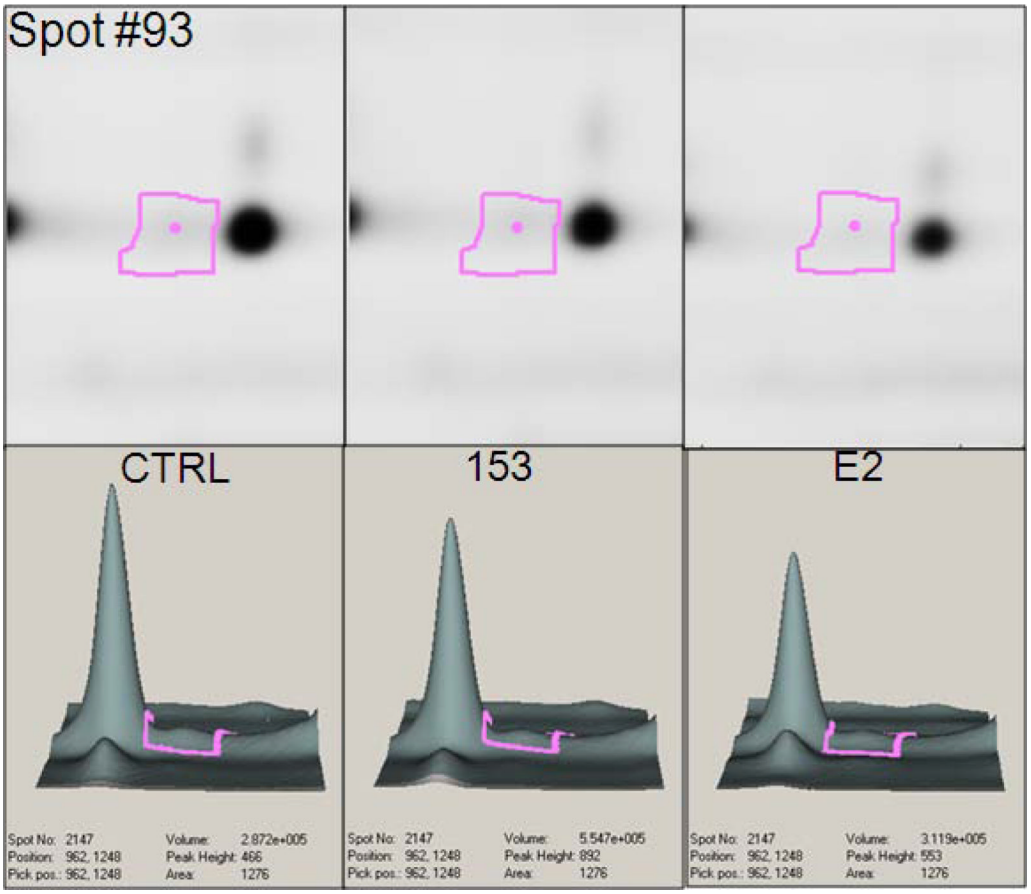

Figure 3.
Gel visualization of selected spots from DeCyder Analysis. Detailed analysis of protein spots, along with 3D images to visualize the protein expression changes. Representative data images show up-regulated and down-regulated spots in the following treatment groups: Control (0.1% DMSO); PCB153 (100ng/ml); 17β-estradiol (1ng/ml).

A

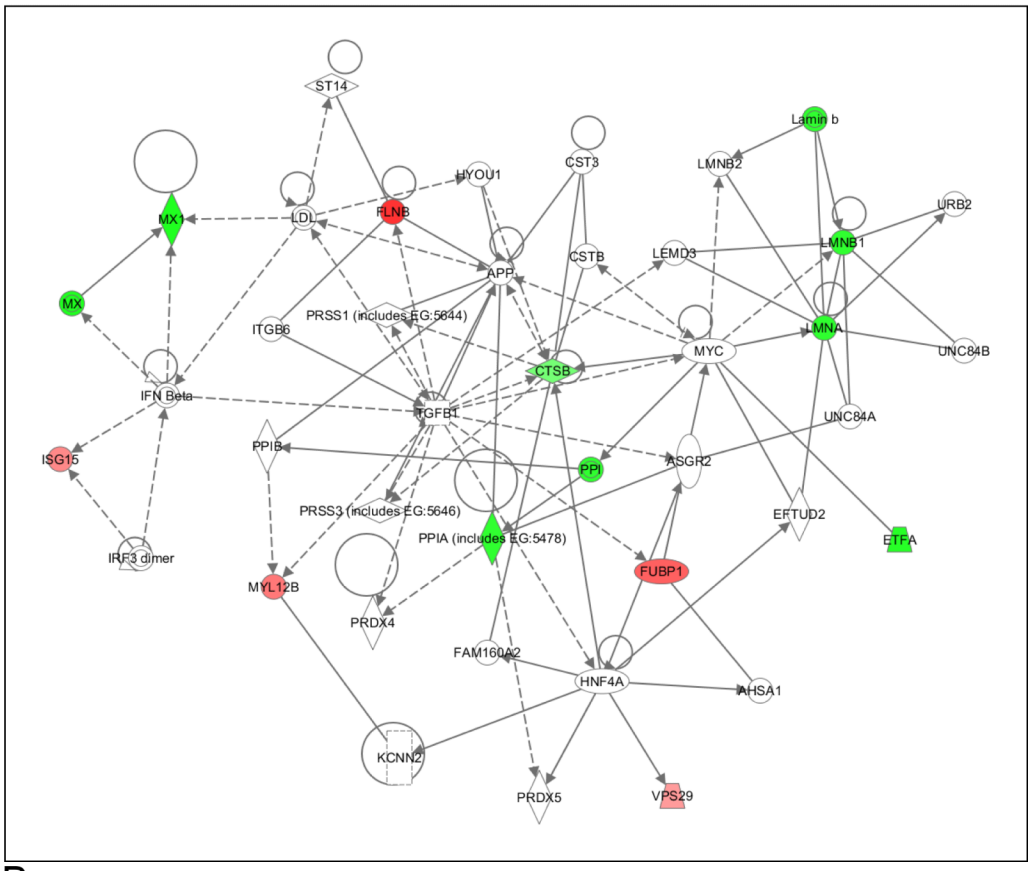

B

Top Bio Functions

Diseases and Disorders

Name	p-value	# Molecules
Antimicrobial Response	6.85E-04 - 4.89E-02	1
Cardiovascular Disease	6.85E-04 - 2.57E-02	1
Dermatological Diseases and Conditions	6.85E-04 - 2.05E-03	1
Developmental Disorder	6.85E-04 - 2.35E-02	3
Genetic Disorder	6.85E-04 - 4.30E-02	5

Molecular and Cellular Functions

Name	p-value	# Molecules
Cell Morphology	2.53E-06 - 2.04E-02	3
Cell Cycle	6.85E-04 - 2.37E-02	2
Cell Death	6.85E-04 - 4.17E-02	7
Cellular Assembly and Organization	6.85E-04 - 2.04E-02	4
DNA Replication, Recombination, and Repair	6.85E-04 - 2.74E-03	2

Physiological System Development and Function

Name	p-value	# Molecules
Cardiovascular System Development and Function	4.22E-07 - 2.30E-02	3
Connective Tissue Development and Function	6.85E-04 - 2.37E-02	1
Nervous System Development and Function	6.85E-04 - 2.05E-03	2
Organismal Development	6.85E-04 - 1.14E-02	2
Tissue Morphology	6.85E-04 - 4.12E-02	3

Figure 4.

Network analysis of identified proteins was performed using Ingenuity Pathways Analysis software (IPA). (A) This illustration represents a merger of the most significant networks regulated by both PCB153 and estradiol. Networks of proteins were algorithmically generated with the IPA software based on their connectivity and assigned a score. Each protein is represented as a node and labeled by its corresponding gene name. Node color intensity indicates the degree of up- (red) or down- (green) regulation by PCB153 and estradiol treatments. A continuous line means a direct relationship between the two proteins, whereas a discontinuous line indicates an indirect association. (B) A summary of the top biological networks identified by IPA.

Table 1
Proteins identified in 2D-gel with density differences ≥ 1.5 fold

Protein spots are shown with the reference spot numbering, molecular weight (MW), and the fold increase or decrease (difference) of the protein spots for comparison between each group. The positive and negative numbers indicate up and down-regulated proteins, respectively. The DeCyder spot detection algorithm calculated ratio (volume of a spot from the secondary image/volume of the corresponding spot from the primary image), and a threshold of 1.5 fold change was set.

Protein ID	Spot No.	PCB153 vs Control difference	Estradiol vs Control difference	Estradiol vs PCB153 difference
1	166	1.66	-1.70	-2.83
2	439	-1.18	1.53	1.80
3	353	1.06	1.62	1.52
4	15	-1.10	2.08	2.29
5	48	-1.23	2.23	2.74
***6**	**102**	**-1.24**	**2.30**	**2.85**
7	141	1.62	-1.57	-2.56
8	280	-1.03	1.63	1.68
9	364	1.43	2.31	1.61
10	430	1.06	2.12	2.00
11	455	1.50	1.39	-1.08
12	369	1.07	-1.65	-1.78
13	526	1.01	-1.94	-1.97
14	416	1.20	-1.58	-1.90
15	428	1.17	-1.79	-2.08
16	819	-1.56	-1.68	-1.08
17	831	-1.94	-1.56	1.24
18	840	-2.22	1.13	2.50
19	948	-1.56	-1.10	1.42
20	812	-1.76	-1.79	-1.02
***21**	**772**	**1.85**	**-1.60**	**-2.96**
22	705	1.01	1.93	1.91
23	631	-2.00	1.10	2.19
***24**	**648**	**-2.96**	**-1.73**	**1.71**
25	829	1.14	1.50	1.31
26	822	1.03	1.62	1.56
27	868	-1.13	1.61	1.81
28	775	1.09	1.55	1.42
29	621	-1.69	-1.45	1.16
***30**	**642**	**-1.64**	**-1.61**	**1.02**
31	701	1.28	2.30	1.80
32	640	-1.17	-1.51	-1.29
33	693	1.71	3.14	1.83

Protein ID	Spot No.	PCB153 vs Control difference	Estradiol vs Control difference	Estradiol vs PCB153 difference
***34**	**702**	**1.76**	**1.79**	**1.02**
35	732	1.04	1.06	1.02
36	816	-1.04	-1.57	-1.52
37	734	-1.05	1.63	1.71
38	1300	-1.53	1.25	1.91
39	1339	-1.57	1.21	1.91
40	1235	1.13	1.53	1.36
41	1150	1.04	1.66	1.60
42	367	1.01	1.72	1.70
43	991	1.22	-1.51	-1.84
44	1068	1.08	1.81	1.67
45	1045	-1.04	1.81	1.88
46	1191	1.49	-1.62	-2.42
47	1318	1.09	1.60	1.46
48	1303	-1.11	-1.80	-1.63
49	1353	-1.03	1.66	1.70
50	1469	1.33	2.73	2.05
51	1129	-1.23	1.71	2.10
52	978	-1.00	1.62	1.62
53	969	1.10	1.98	1.80
54	1049	-1.02	-1.52	-1.49
55	989	-1.22	1.50	1.83
56	1020	-1.20	1.66	1.99
57	998	-1.17	1.71	2.00
58	1178	1.01	-1.53	-1.54
59	1225	-1.03	-1.88	-1.84
60	1367	-1.01	-1.52	-1.50
61	1428	1.06	-1.58	-1.68
62	1283	1.02	1.52	1.49
63	1366	1.28	1.78	1.39
64	1423	-1.02	-2.64	-2.58
65	1427	1.13	-2.51	-2.83
66	1440	1.04	-1.47	-1.53
67	1488	-1.04	-2.45	-2.36
68	1175	-1.12	-1.73	-1.54
69	1557	-1.03	-1.66	-1.61
70	1649	-1.06	1.50	1.59
71	1795	-1.11	1.66	1.84
***72**	**1859**	**-2.04**	**-1.07**	**1.91**

Protein ID	Spot No.	PCB153 vs Control difference	Estradiol vs Control difference	Estradiol vs PCB153 difference
73	1882	-1.90	1.22	2.32
74	1884	-1.64	-1.33	1.24
75	1831	-1.12	1.47	1.65
76	1589	-1.13	1.73	1.95
77	1626	-1.27	1.26	1.60
78	1628	-1.05	-1.51	-1.44
***79**	**1623**	**-1.27**	**-1.67**	**-1.32**
80	1613	-1.18	-1.63	-1.38
81	1894	1.34	1.51	1.13
82	1757	-1.21	1.70	2.05
83	1763	-1.09	1.87	2.03
84	1774	-1.06	1.80	1.91
***85**	**2007**	**1.96**	**1.12**	**-1.76**
86	2038	-1.42	1.46	2.07
***87**	**2059**	**-2.44**	**1.52**	**3.70**
88	2125	-1.51	1.12	1.69
89	2084	1.16	-1.61	-1.87
90	2249	-1.63	-1.53	1.07
91	2051	1.00	1.93	1.93
***92**	**2208**	**-1.51**	**1.33**	**2.00**
***93**	**2147**	**-1.09**	**-1.60**	**-1.47**
94	2088	1.13	-1.66	-1.87
95	2098	-1.76	1.29	2.27
96	2237	-1.17	-1.82	-1.55

Table 2

Protein identification by mass spectrometry

The spots of interest were picked up by Ettan Spot Picker and digested in-gel with modified porcine trypsin protease. The digested tryptic peptides were desalted, peptides eluted, and spotted on the MALDI plate. Protein identification was based on peptide fingerprint mass mapping (using MS spectra) and peptide fragmentation mapping (using MS/MS spectra). Combined MS and MS/MS spectra are submitted for database search using GPS Explorer software equipped with the MASCOT search engine to identify proteins from the database of National Center for Biotechnology Information non-redundant (NCBInr). Candidates with either protein score confidence interval (C.I.) % or Ion C.I.% greater than 95 were considered significant.

Spot number	Top Ranked Protein Name(Species)	Location*	Type(s)*	Accession No.	Protein MW	Protein PI	Pep.Count	Protein Score	Protein Score C. I. %	Total Ion Score	Total Ion C. I. %
6	filamin B [Homo sapiens]	Cytoplasm	other	gi|9664263	71134.8	6.25	10	88	99.963	26	0
21	Lamin B1 [Homo sapiens]	Nucleus	other	gi|15126742	66366.6	5.13	9	77	99.595	45	97.636
24	MX1 protein [Homo sapiens]	Nucleus	enzyme	gi|40225574	66810.8	5.9	9	80	99.756	23	0
30	lamin A/C transcript variant 1 [Homo sapiens]	Nucleus	other	gi|57014047	74025.6	6.44	33	443	100	150	100
34	far upstream element-binding protein [Homo sapiens]	Nucleus	transcription regulator	gi|17402900	67518.5	7.18	13	132	100	47	98.289
72	cathepsin B	Cytoplasm	peptidase	gi|741376	17143	5.44	7	327	100	259	100
79	Chain A, Human Electron Transfer Flavoprotein	Cytoplasm	transporter	gi|2781202	33075.4	6.95	11	188	100	94	100
85	vacuolar protein sorting 29 isoform 1 [Homo sapiens]	Cytoplasm	transporter	gi|7706441	20492.7	6.29	9	186	100	92	100
87	myosin regulatory light chain MRCL2 isoform A [Homo sapiens]	Cytoplasm	other	gi|15809016	19766.5	4.71	10	475	100	346	100
92	ISG15 ubiquitin-like modifier [Homo sapiens]	Cytoplasm	other	gi|14550514	17903.3	6.84	5	290	100	228	100
93	Chain A, Cyclophilin A	Cytoplasm	enzyme	gi|1633054	17869.8	7.82	10	340	100	225	100

Cell Biol Toxicol. Author manuscript; available in PMC 2011 November 30.

Spot number	Top Ranked Protein Name(Species)	Location*	Type(s)*	Accession No.	Protein MW	Protein PI	Pep.Count	Protein Score	Protein Score C. I. %	Total Ion Score	Total Ion C. I. %
	Complexed With Dipeptide Gly-Pro										

*Protein Location and Type were identified using Ingenuity Pathways Analysis software (Ingenuity Systems).

Table 3

Up and Down regulated proteins

The table displays differentially expressed proteins following PCB153 and estradiol treatment. The positive and negative numbers indicate Up- (red) and Down (green)-regulated proteins, respectively.

Spot number	Gene Symbol	PCB153 / DMSO	Estradiol / DMSO	Estradiol / PCB153
6	FLNB	-1.24	2.30	2.85
21	LMNB1	1.85	-1.60	-2.96
24	MX1	-2.96	-1.73	1.71
30	LMNA	-1.64	-1.61	1.02
34	FUBP1	1.76	1.79	1.02
72	CTSB	-2.04	-1.07	1.91
79	ETFA	-1.27	-1.67	-1.32
85	VPS29	1.96	1.12	-1.76
87	MYL12B	-2.44	1.52	3.70
92	ISG15	-1.51	1.33	2.00
93	PPIA	-1.09	-1.60	-1.47